Journal of Orthopaedic Translation 23 (2020) 67–76

Contents lists available at ScienceDirect

Journal of Orthopaedic Translation

journal homepage: www.journals.elsevier.com/journal-of-orthopaedic-translation

Original Article

Hepcidin deficiency causes bone loss through interfering with the canonical Wnt/β-catenin pathway via Forkhead box O3a

Guangfei Li [a,b,☆], Hui Zhang [a,b,☆], Jiadong Wu [c,☆], Aifei Wang [a,b], Fan Yang [a,b], Bin Chen [a,b], Yan Gao [a,b], Xiaowei Ma [d], Youjia Xu [a,b,*]

[a] Department of Orthopaedics, The Second Affiliated Hospital of Soochow University, 215004, Suzhou, China
[b] Osteoporosis Institute of Soochow University, 1055 Sanxiang Road, 215004, Suzhou, China
[c] Department of Orthopaedics, The Affiliated Yancheng Hospital of Southeast University Medical College, 224005, Yancheng, China
[d] Department of Orthopaedics, Zhongshan Hospital of Dalian University, 116001, Dalian, China

ARTICLE INFO

Keywords:
Forkhead box O3a
Hepcidin
Osteoblasts
Osteoclasts
Osteoporosis
Wnt/β-catenin pathway

ABSTRACT

Objective: Hepcidin deficiency is known to cause body iron accumulation and bone microarchitecture defects, but the exact underlying mechanisms of hepcidin deficiency-induced bone loss remain unclear. Our objective was to understand the molecular mechanism of hepcidin deficiency-induced bone loss.

Methods: The bone phenotypes of wild type (WT) and hepcidin knockout (Hepcidin-KO) mice were measured by microcomputed tomography. The osteoclastic marker of the bone was measured by tartrate-resistant acid phosphatase staining. The osteoblastic marker of the bone was measured by immunostaining of osteocalcin. Primary osteoblastic and osteoclastic differentiation was performed using bone marrow cells. The mature osteoclast was determined by tartrate-resistant acid phosphatase staining, pit formation assay and relative gene expression. The mature osteoblast was determined by alkaline phosphatase activity, alkaline phosphatase staining, Alizarin Red staining and relative gene expression. The protein expression of β-catenin, TCF4/TCF7L2 and Forkhead box O3a (FOXO3a) was measured by Western blot and their combination by co-immunoprecipitation. *In vivo* study was performed by tail vein administration of FOXO3a-RNAi using an adeno-associated virus in Hepcidin-KO mice.

Results: We found that Hepcidin-KO mice exhibited iron accumulation and bone loss compared with WT mice. The osteoclastic differentiation of bone marrow-derived macrophages from Hepcidin-KO mice was not significantly different from that of bone marrow–derived macrophages from WT mice. However, the osteoblastic differentiation of bone marrow–derived mesenchymal stem cells from Hepcidin-KO mice was obviously decreased compared with that of bone marrow–derived mesenchymal stem cells from WT mice. Furthermore, it was confirmed in this study that upon hepcidin deficiency, β-catenin, TCF4/TCF7L2 and FOXO3a expression in bone tissues was not altered, but β-catenin combination with TCF4/TCF7L2 was strongly inhibited by β-catenin combination with FOXO3a, indicating that the canonical Wnt/β-catenin pathway was affected. Tail vein administration of FOXO3a-RNAi using an adeno-associated virus in Hepcidin-KO mice resulted in bone mass recovery.

Conclusion: These findings suggested that hepcidin deficiency might cause bone loss by interfering with the canonical Wnt/β-catenin pathway via FOXO3a, and FOXO3a inhibition would be a possible approach to treat hepcidin deficiency-induced bone loss.

The translational potential of this article: Hepcidin deficiency, as well as iron accumulation, has been considered as a risk factor for osteoporosis. For this kind of osteoporosis, inhibition of FOXO3a either by neutralized antibody or AAV-mediated RNAi, represents an effective and promising method.

* Corresponding author. Department of Orthopaedics, The Second Affiliated Hospital of Soochow University, 215004, Suzhou, China.
E-mail address: xuyoujia@suda.edu.cn (Y. Xu).
☆ Guangfei Li, Hui Zhang and Jiadong Wu contributed equally to this article and should be considered as first authors.

https://doi.org/10.1016/j.jot.2020.03.012
Received 22 August 2019; Received in revised form 1 March 2020; Accepted 23 March 2020
Available online 21 April 2020

Introduction

Iron accumulation has been reported to be associated with osteoporosis and is thought to be an independent risk factor of osteoporosis [1–3]. Postmenopausal osteoporosis, which was previously believed to be due to estrogen deficiency, is now also considered to be the result of iron accumulation [4–6]. The serum ferritin concentration increases when the estrogen level decreases in females during ageing after approximately 45 years, which is a perimenopausal period [7]. During a long-duration space flight on the International Space Station, serum ferritin and body iron levels were shown to be increased early in flight, and serum ferritin was positively correlated with a hip bone mineral density (BMD) decrease [8].

Iron chelators, such as desferrioxamine [9–11], deferasirox [12] and lactoferrin [13], were all reported to promote osteogenesis and increase bone mass, which are beneficial for both osteoporosis and fracture healing.

To better understand the role of iron metabolism in bone metabolism, we used a mouse model of hepcidin knockout (Hepcidin-KO) mice. Hepcidin is an endogenous hormone peptide and has been found to be the main regulator of iron homeostasis [14–16]. Hepcidin binds to ferroportin located on enterocytes. The combination of hepcidin and ferroportin could reduce ferroportin activity, which in turn inhibits iron uptake and transfer from the gastrointestinal system to the circulatory system, leading to decreased body iron content [17,18]. As previously reported, when hepcidin was deficient in mice, iron accumulated in the body, bone microarchitecture defects were obvious and bone load-bearing capacity was undermined [19,20]. However, the molecular mechanism of hepcidin deficiency–induced bone loss remains unclear.

In this study, we tested the osteoblastic differentiation of bone marrow–derived mesenchymal stem cells (BMSCs) and the osteoclastic differentiation of bone marrow–derived macrophages (BMMs) from wild type (WT) and Hepcidin-KO mice to determine which is responsible for hepcidin deficiency–induced bone abnormalities. Furthermore, we studied the role of Forkhead box O3a (FOXO3a), which is known to affect the canonical Wnt/β-catenin signalling pathway, in the process of bone loss caused by hepcidin deficiency.

Materials and methods

Experimental animals

Six-month-old WT and Hepcidin-KO ($Hamp^{-/-}$) male mice were provided by the Cambridge-Soochow University Genome Resource Center. The mice on a C57Bl/6J background were maintained and bred in a specific pathogen-free laboratory with a controlled temperature (25°C) at Soochow University. The relative humidity was around 50%, and the mice were kept under 12 h light/12 h dark cycles. The mice have free access to water and food. There were six mice in each animal group. All animal experiments were performed in accordance with institutional guidelines and approved by the Ethics Committee of Soochow University.

Table 1
Primers used for quantitative reverse transcription-PCR.

Gene	Primers (Forward/Reverse)
Mcsfr	(F) 5′- GGTGGCTGTGAAGATGCTAA -3′
	(R) 5′- AGGTCCTCCGTGAGTACAGG -3′
Nfatc1	(F) 5′- ATACCTGGCTCGGTAACACC -3′
	(R) 5′- CATGCTCCAGTGCTGTCTTT -3′
Cathepsin K	(F) 5′- CAGCAGAACGGAGGCATTGA -3′
	(R) 5′′- CTTTGCCGTGGCGTTATACATACA -3'
TRAP	(F) 5'- TTGCGACCATTGTTAGCCACATA -3'
	(R) 5'- TCAGATCCATAGTGAAACCGCAAG -3'
Runx2	(F) 5'- TCGGAGAGGTACCAGATGGG -3'
	(R) 5'- AGGTGAAACTCTTGCCTCGT -3'
ALP	(F) 5'- GCTGATCATTCCCACGTTTT -3'
	(R) 5'- ACCATATAGGATGGCCGTGA -3'
Osx	(F) 5'- GCTCGTAGATTTCTATCCTC -3'
	(R) 5'- CTTAGTGACTGCCTAACAGAGA -3'
Col1	(F) 5'- TGACTGGAAGAGCGGAGAGTA -3'
	(R) 5'- GACGGCTGAGTAGGGAACAC -3'
FOXO3a	(F) 5'- TAGGCTGCACTGGGGGGTAA -3'
	(R) 5'- ACTGATCAGAGCTACAAGAC -3′
GAPDH	(F) 5′- AGAACATCATCCCTGCATCC -3′
	(R) 5′- AGTTGCTGTTGAAGTCGC -3′

Bone specimen processing

The femurs and tibias of the mice were obtained after removing the adjacent muscle and soft tissue under a hood. The femurs were fixed in a 10% formalin solution for 48 h and used for microcomputed tomography (micro-CT) detection. Then, after micro-CT, the femurs were decalcified in a 10% ethylenediaminetetraacetic acid solution for 30 days and embedded in a paraffin solution. The paraffinised specimens were sectioned to 5-μm-thick sections with a sliding microtome. Then, one section selected randomly from every five sections was stained with tartrate-resistant acid phosphatase (TRAP) solution and immunostained with osteocalcin (OCN). The tibias were flushed to be used for primary osteoblast cell culture and osteoclast differentiation.

Micro-CT scanning

Femurs were placed in a sample holder with gauze and scanned with a micro-CT machine (Skyscan 1176, Belgium) using a 9-μm resolution, 50 kV, 500 μA and 0.5° rotation step. A trabecular bone analysis was performed on the distal femurs. Analytic indices included the BMD, bone volume over total volume (BV/TV) ratio, trabecular number (Tb.N), trabecular separation (Tb.Sp) and trabecular thickness (Tb.Th). The calculation methods for the bone parameters have been previously described [21].

Bone immunohistology

Randomly selected sectioned samples were hydrated in alcohol with descending concentrations, followed by xylene deparaffinisation. Then, the samples were reacted with 1x target retrieval solution at 65°C for 1 h to expose the antigenic sites. Next, the samples were rinsed with 1x phosphate-buffered saline (PBS) and analysed after pretreatment with a 1% peroxide-methanol solution for 30 min to quench endogenous peroxidase activity. After that, the samples were incubated with diluted 1x PBS with 5% normal bovine serum, 0.3% Triton X-100 and 1% bovine serum albumin at 37°C for 1 h to avoid nonspecific immune reactions to antigens. The specimens thereafter were reacted with diluted primary anti-osteocalcin antibody (OCN, 1:50) for 12 h at 4°C and rinsed with PBS. The sections then were incubated with the secondary antibody biotinylated anti-mouse immunoglobulin G (IgG) (1:200) for 1 h at 37°C and reacted with mixed liquid.

Bone section TRAP staining

Sectioned samples were stained with a TRAP staining solution at 37°C for 10 min. The TRAP staining solution is composed of 0.3 mg/ml fast red violet LB, 50 mM sodium acetate, 100 mg/ml naphthol AS-MX phosphate, 0.1% Triton X-100 and 30 mM sodium tartrate.

Primary BMM culture

BMMs were prepared as reported previously [22]. Murine bone marrow cells were obtained by flushing the tibias and then cultured in α-Minimum Essential Medium (α-MEM) (Invitrogen, Carlsbad, CA, USA) for 24 h with 10% fetal bovine serum (FBS) and macrophage colony-stimulating factor (M-CSF) (10 ng/ml; PeproTech, Rocky Hill, NJ, USA). Nonadherent cells were then collected and cultured for 3 days in

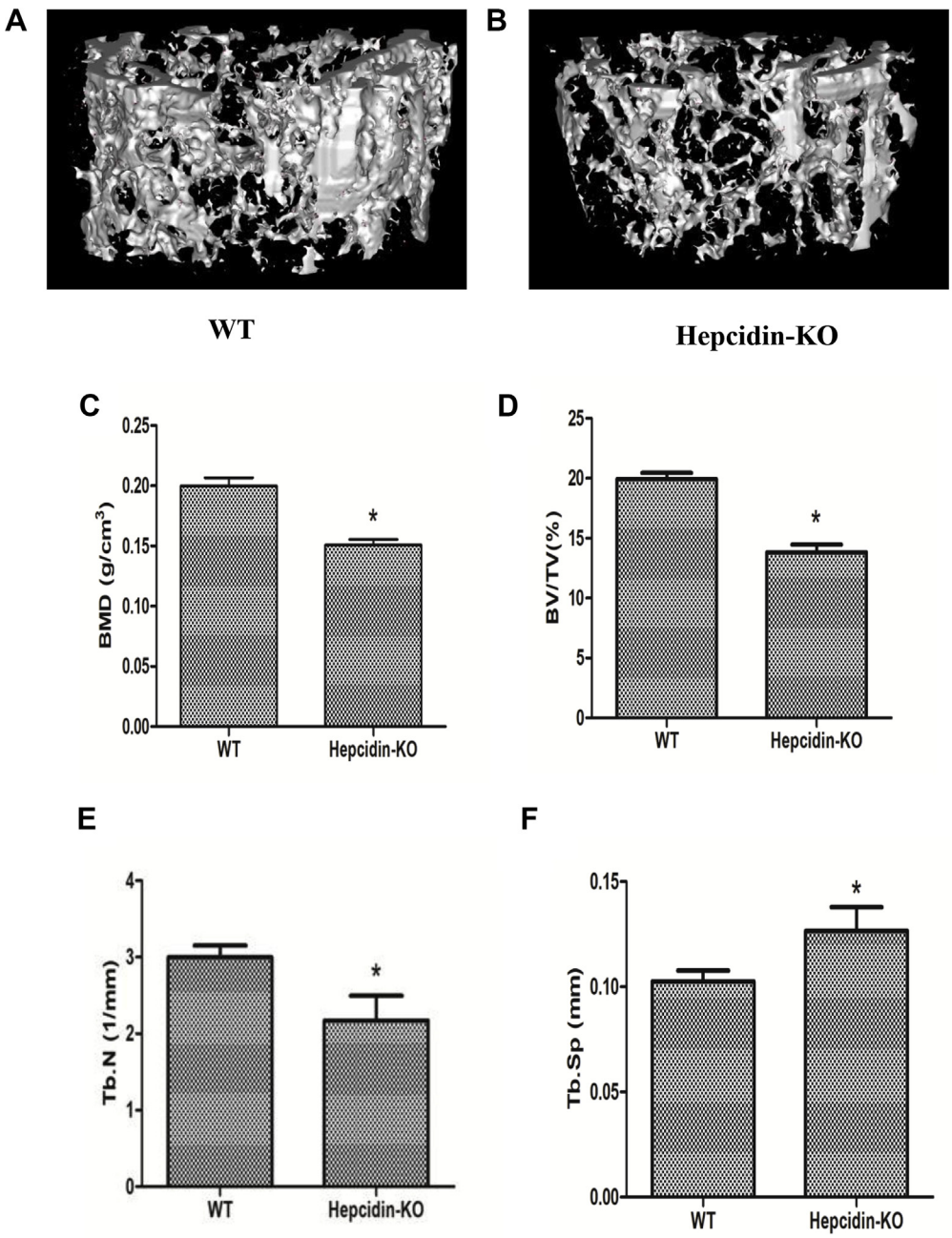

Figure 1. Micro-CT analysis of the trabecular bone of the distal femur from WT and Hepcidin-KO mice at 6 months of age. (A) Representative three-dimensional image of the trabecular bone of the distal femur from WT mice; (B) representative three-dimensional image of the trabecular bone of the distal femur from Hepcidin-KO mice; (C) bone mineral density (BMD); (D) bone volume versus total volume (BV/TV) ratio of the distal femur from WT and Hepcidin-KO mice; (E) trabecular number (Tb.N) of the distal femur from WT and Hepcidin-KO mice; (F) trabecular separation (Tb.Sp) of the distal femur from WT and Hepcidin-KO mice; (G) TRAP staining of distal femur sections from WT; (H) TRAP staining of distal femur sections from Hepcidin-KO mice; (I-J) Magnified views of the projected areas indicated by the black box in G-H; (M) OCN expression in distal femur sections from WT; (N) OCN expression in distal femur sections from Hepcidin-KO mice; (O-P) Magnified views of the projected areas indicated by the black box in M-N; (K) quantification of TRAP+ OCs per bone surface; (L) quantification of the mean intensity for the OCN immunostaining. Data are means ± SD from six mice. *$p < 0.05$ by Student t test. NS = not significant; WT = wild type; Hepcidin-KO = hepcidin knockout; OCN = osteocalcin; Micro-CT = microcomputed tomography.

α-MEM with 10% FBS and M-CSF (30 ng/ml). The adherent cells after 3 days of culture were used as BMMs.

Determination of osteoclastic differentiation

BMMs (1×10^5 cells/cm^2) were cultured in medium supplemented with 30 ng/ml M-CSF and 100 ng/ml receptor activator of nuclear factor kappa-B ligand (RANKL). The cells were collected at 48 h to determine osteoclastic differentiation by measuring the messenger RNA (mRNA) expression of osteoclastic markers (Nfatc1, cathepsin K, Mcsfr and TRAP). As for TRAP staining, cells at 4 days were fixed at room temperature with 4% formaldehyde for 30 min. The cells were washed with PBS twice and then stained with a TRAP staining solution at 37°C for 30 min. TRAP-positive multinucleated cells with more than three nuclei were counted. As for the pit formation assay, BMMs were seeded in Osteo Assay Surface 24-well plates (Corning, NY, USA) at a density of

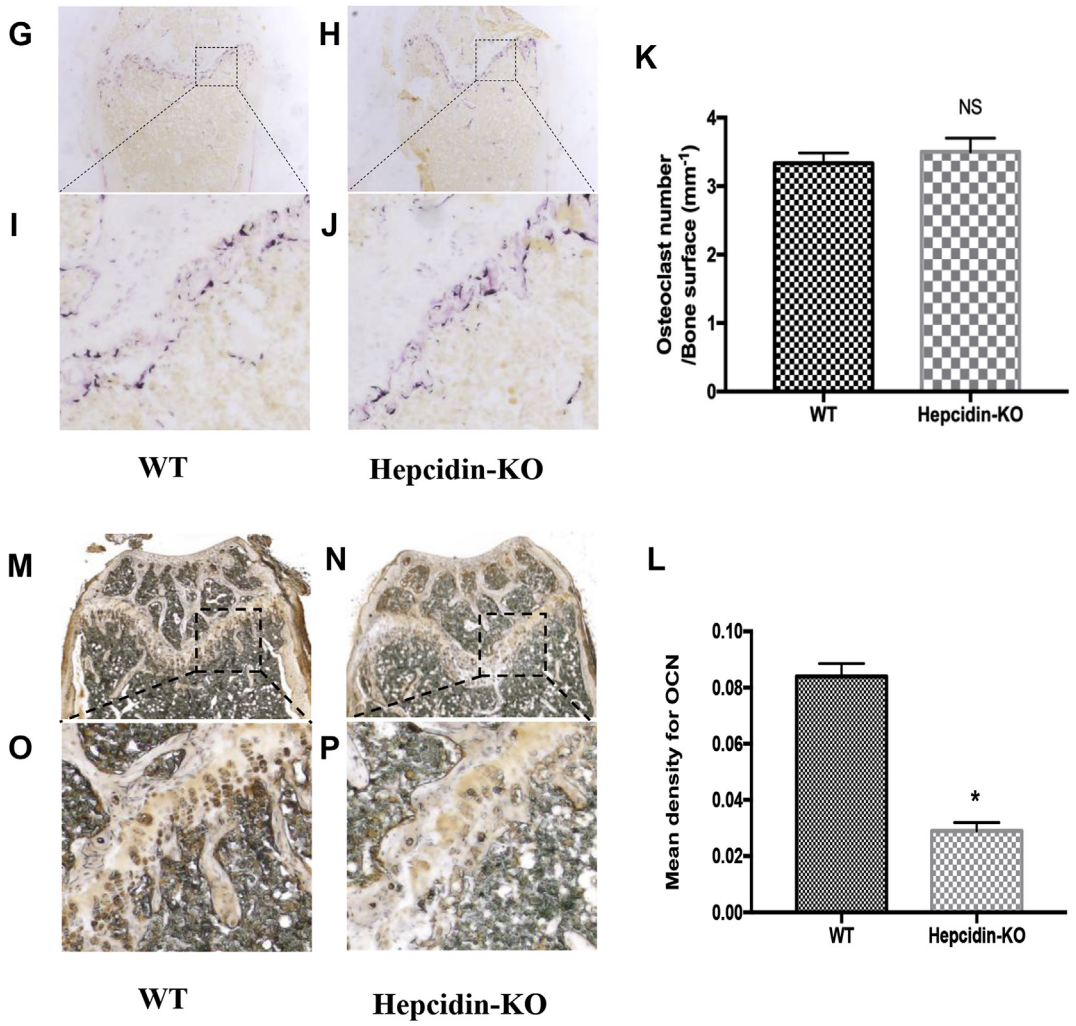

Figure 1. (*continued*).

2.5×10^4 cells/well and then cultured in medium supplemented with M-CSF (30 ng/ml) and RANKL (100 ng/ml) for 4 days. The media was then removed from the wells, and 100 μL of a 10% bleach solution was added. The cells were incubated with the bleach solution at room temperature for 5 min. Then, the wells were washed twice with distilled water and dried at room temperature for 5 h. Individual pits or multiple pit clusters were observed by a microscope at 100× magnification. The ratio of the resorbed area to the total area was calculated using ImageJ software.

Quantitative reverse transcription-polymerase chain reaction analysis

The total RNA was extracted using TRIzol reagent from cells and reverse transcribed into complementary DNA (cDNA) using a commercial kit (Invitrogen). Polymerase chain reaction (PCR) assays were performed with a total reaction volume of 10 μL: 2 × Taq PCR mix (5 μL), nuclease-free water (4 μL), cDNA (0.5 μL) and forward or reverse primers (0.5 μL. PCR conditions were as follows: 94°C for 20 s, 58°C for 30 s and 72°C for 30 s for 38 cycles. The details of the primer sequences are shown in Table 1.

Primary BMSC culture

BMSCs were prepared as described previously [23]. Bone marrow cells were obtained by flushing the tibias and then cultured for 24 h in α-MEM with 10% FBS and M-CSF (10 ng/ml). Nonadherent cells were removed, and the adherent cells were continuously cultured with fresh medium. When the primary cultures become almost confluent, the cells were treated with 0.5 ml of 0.25% trypsin for 2 min at room temperature. The adherent cells after 3 weeks of culture were used as BMSCs.

Determination of osteoblastic differentiation

For alkaline phosphatase (ALP) activity, the cells were treated in accordance with the instructions of the kit (Nanjing Jiancheng Bioengineering Institute, Jiangsu, China). For ALP staining, the cells were fixed with 70% ethanol, incubated with 1% N,N-dimethyl formamide, 0.01% naphthol, AS-MX phosphate and 0.06% fast blue BB for 15 min. For Alizarin Red staining, cells were washed with PBS and fixed with 10% paraformaldehyde. After washing, cells were stained with 40 mM freshly Alizarin Red solution (PH = 4.2) and incubated for 10 min at room temperature. Alizarin was aspirated, and the wells were washed at least 3 times before observation. Calcium deposits can be visualised by red colour. To quantify the staining, cultures were destained using 10% cetylpyridinium chloride in 10 mM sodium phosphate, pH7.0, for 15 min at room temperature. Aliquots of exacts were diluted 10-fold in 10% cetylpyridinium chloride solution, and Alizarin Red concentration was determined by absorbance measurement at 562 nM.

Western blot analysis and co-immunoprecipitation

Cells were washed with PBS and lysed with

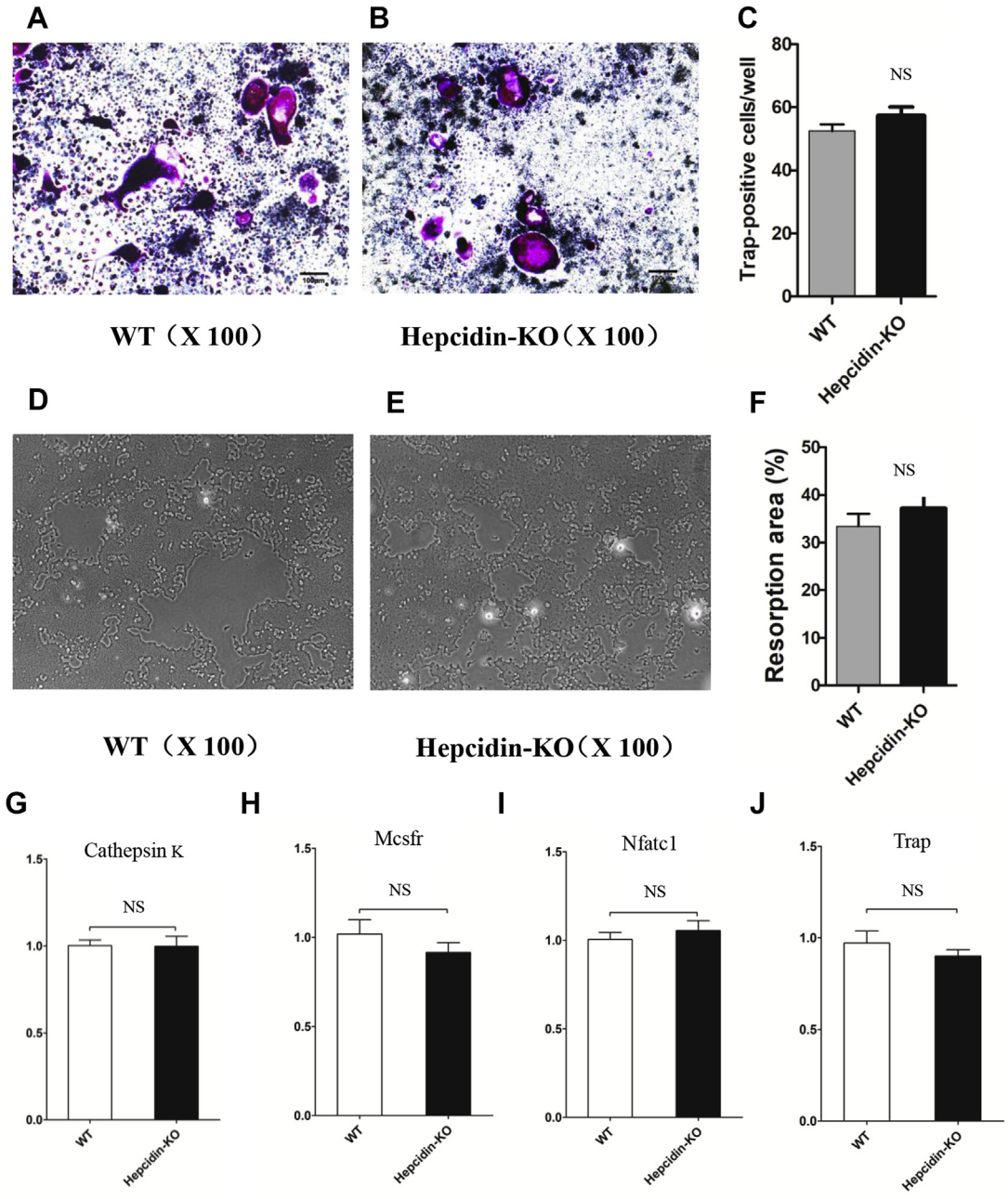

Figure 2. Hepcidin deficiency does not alter osteoclastic differentiation or activity. (A) Representative images of TRAP-positive cells (a marker of mature osteoclasts) differentiated from the BMMs of WT mice; (B) representative images of TRAP-positive cells (a marker of mature osteoclasts) differentiated from the BMMs of Hepcidin-KO mice; (C) statistical analysis of the number of TRAP-positive cells from the BMMs of WT and Hepcidin-KO mice. (D) Representative images of the resorption pits of mature osteoclasts from the BMMs of WT mice; (E) representative images of the resorption pits of mature osteoclasts from the BMMs of Hepcidin-KO mice; (F) statistical analysis of the resorption area of mature osteoclasts from the BMMs of WT and Hepcidin-KO mice; (G) mRNA expression of the osteoclastic markers cathepsin K; (H) mRNA expression of the osteoclastic marker Mcsfr; (I) mRNA expression of the osteoclastic markers Nfatc1; (J) mRNA expression of the osteoclastic markers TRAP during osteoclastic differentiation. Data are means ± SD from six mice. NS = not significant; WT = wild type; Hepcidin-KO = hepcidin knockout; BMM = bone marrow–derived macrophage.

radioimmunoprecipitation assay lysis buffer. Protein was assessed with a bicinchoninic acid Protein Assay Kit (Beyotime, Beijing, China). 40 mg total protein was mixed with 5× sodium dodecyl sulfate–polyacrylamide gel electrophoresis sample loading buffer, boiled for 5 min at 100°C and loaded onto sodium dodecyl sulfate–polyacrylamide gel electrophoresis gels. Afterwards, the proteins were subjected to sodium dodecyl sulfate electrophoresis at 120 V for 2 h and transferred to polyvinylidene difluoride membrane by electroblotting at 330 mA for 60 min. The membranes were then blocked with 5% nonfat milk in tris-buffered saline containing 0.1% Tween 20 (TBST) for 1 h, washed with TBST, incubated with primary antibody diluted in TBST at room temperature for 2 h. Again, the membranes were washed with TBST and incubated for 1 h with the appropriate horseradish peroxidase–conjugated secondary antibody. Co-immunoprecipitation was performed as described previously [24]. The primary antibodies used in this experiment were as follows: antibodies against β-catenin (BD Biosciences, Franklin Lakes, NJ, USA), antibodies against glyceraldehyde 3-phosphate dehydrogenase (Abcam, Cambridge, United Kingdom), antibodies against TCF4/TCF7L2

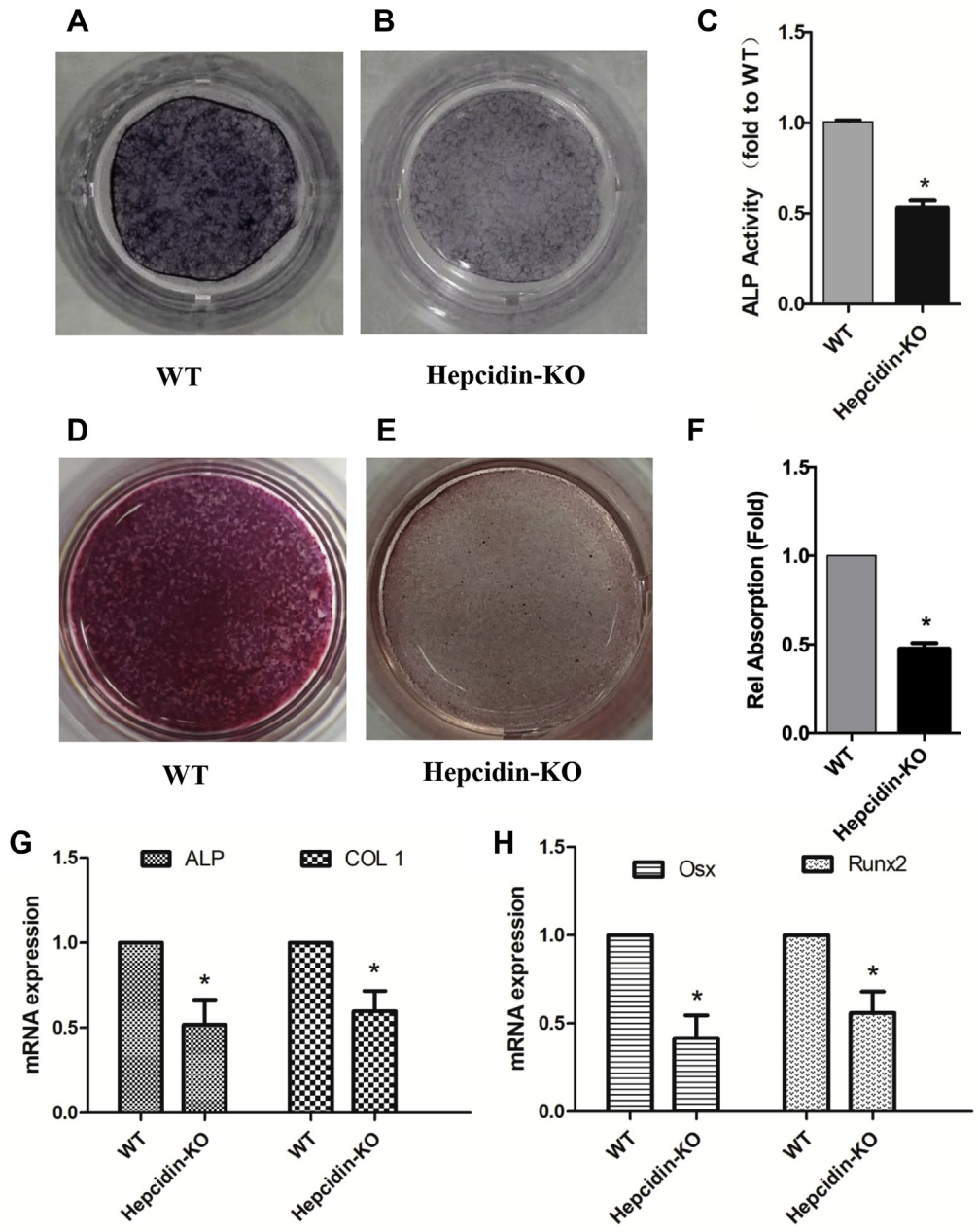

Figure 3. Hepcidin deficiency inhibits osteoblastic differentiation and activity. (A) Representative images of ALP staining of osteoblasts differentiated from the BMSCs of WT mice; (B) representative images of ALP staining of osteoblasts differentiated from the BMSCs of Hepcidin-KO mice; (C) ALP activity of osteoblasts differentiated from the BMSCs of WT and Hepcidin-KO mice; (D) representative images of Alizarin Red staining of osteoblasts differentiated from the BMSCs of WT mice; (E) representative images of Alizarin Red staining of osteoblasts differentiated from the BMSCs of Hepcidin-KO mice; (F) the intensity of Alizarin Red staining was quantified with 10% CPC; (G-H) mRNA expression of the osteoblastic markers ALP, COL 1, Osx and Runx2 during osteoblastic differentiation. Data are means ± SD from six mice. *$p < 0.05$ by Student*t* test. ALP = alkaline phosphatase; CPC = cetylpyridinium chloride; WT = wild type; Hepcidin-KO = hepcidin knockout; BMSC = bone marrow–derived mesenchymal stem cell.

(Cell Signaling Technology, Danvers, MA, USA), antibodies against β-actin, FOXO3a and normal mouse IgG (Santa Cruz Biotechnology, Dallas, TX, USA).

Adeno-associated virus vector construction and delivery

The adeno-associated virus (AAV) vectors GV487 (U6-MCS-CAG-EGFP) expressing mouse FOXO3a short hairpin RNA (shRNA) (5′-GCTCTTGGTGGATCATCAA-3′) or control shRNA (5′-CGCTGAG-TACTTCGAAATGTC-3′) were constructed by Genechem (Shanghai, China). The AAV vectors were administered by tail vein injection (100 μL total volume) at a dose of 3.86×10^{11} vg per animal in the study group (KO+ FOXO3a-RNAi) using a 30-gauge ultra-fine insulin syringe and at a dose of 4.29×10^{11} vg per animal in the control group (KO+ FOXO3a-NC). One month after this single injection, the mice were euthanised, and their bones were collected for micro-CT scanning. There were six mice in each animal group. All animal experiments were performed in accordance with institutional guidelines and approved by the Ethics Committee of Soochow University.

Statistical analysis

The data are presented as the means ± standard deviation of three independent experiments. The differences between two groups were analysed by Student *t* test using GraphPad Prism Software, version 4.0. A p value < 0.05 was considered statistically significant.

Results

Hepcidin deficiency causes bone loss

To assess the effect of hepcidin deficiency on the bone

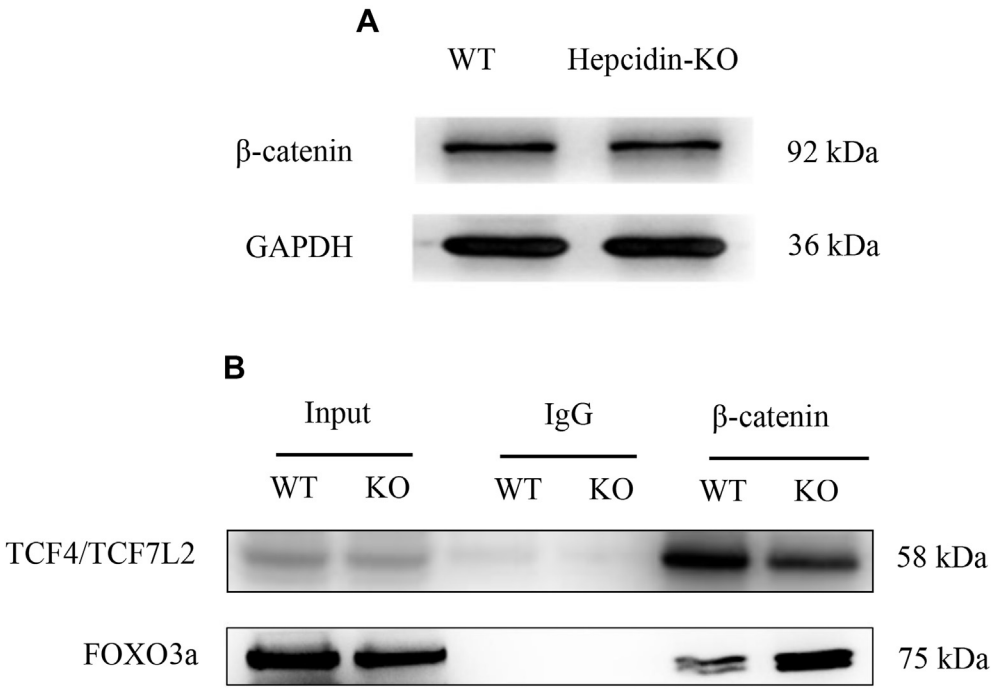

Figure 4. Hepcidin deficiency diverts β-catenin from TCF4/TCF7L2 to FOXO3a. (A) Protein expression of β-catenin in bone tissues from WT and Hepcidin-KO mice according to Western blot; (B) Co-IP analysis of the β-catenin and TCF4/TCF7L2 association and the β-catenin and FOXO3a association in bone tissues from WT and Hepcidin-KO mice. The blots are representative of three independent experiments. Co-IP = co-immunoprecipitation; WT = wild type; Hepcidin-KO = hepcidin knockout; FOXO3a = Forkhead box O3a.

microarchitecture, micro-CT was performed. Micro-CT analysis of the distal femur showed significant bone loss in Hepcidin-KO mice (Fig. 1A) but not in WT mice (Fig. 1B). The BMD (Fig. 1C), BV/TV ratio (Fig. 1D) and Tb.N (Fig. 1E) were all significantly lower in Hepcidin-KO mice than in WT mice. Tb.Sp (Fig. 1F) was increased, and the Tb.Th (data not shown) was not altered in Hepcidin-KO mice compared with that in WT mice. In addition, our group previously reported that hepcidin-KO mice exhibited body iron accumulation [19]. In this study, WT and Hepcidin-KO mice had similar osteoclastic function according to TRAP staining (Fig. 1G–1K), whereas Hepcidin-KO mice exhibited less osteoblastic function as indicated by OCN immunostaining (Fig. 1L–P).

Hepcidin deficiency does not alter osteoclastic differentiation or activity

To test whether hepcidin deficiency–induced bone loss is associated with osteoclastic differentiation and activity, we obtained primary mouse BMMs from the tibia and evaluated the process of osteoclast differentiation in the presence of M-CSF and RANKL. The number of TRAP-positive cells in the BMMs from Hepcidin-KO mice was not significantly different from that of WT mice (Fig. 2A–2C). As indicated by a pit formation assay, the bone resorption area after osteoclast induction was also not significantly altered (Fig. 2D–2F). Consistent with the TRAP staining and pit assay results, there were no significant differences in the mRNA expression of osteoclastic markers, including cathepsin K (Fig. 2G), Mcsfr (Fig. 2H), Nfatc1 (Fig. 2I) and TRAP (Fig. 2J), between the two groups. Therefore, hepcidin deficiency-induced bone loss is not associated with osteoclastic differentiation.

Hepcidin deficiency inhibits osteoblastic differentiation and activity

To ascertain whether hepcidin deficiency–induced bone loss is associated with osteoblastic differentiation and activity, we obtained primary mouse BMSCs from the tibia and evaluated the process of osteoblast differentiation in the presence of osteogenic culture medium. ALP staining and Alizarin Red staining showed that hepcidin deficiency inhibited osteoblastic differentiation (Fig. 3A–3B, Fig. 3D–3F), and an ALP activity analysis showed that hepcidin deficiency inhibited osteoblastic activity (Fig. 3C). Consistent with the ALP staining, Alizarin Red staining and ALP activity assay results, mRNA expression of the osteoblastic markers ALP, collagen type 1 (COL1), osterix (Osx) and runt-related transcription factor 2 (Runx2) was significantly lower in the Hepcidin-KO group than in the WT group (Fig. 3G and 3H). Therefore, bone loss caused by hepcidin deficiency may be because of reduced osteoblastic differentiation and activity in the absence of hepcidin.

Hepcidin deficiency diverts β-catenin from T-cell factor (TCF4/TCF7L2) to FOXO3a

To further determine why hepcidin deficiency inhibited osteoblastic differentiation and activity, the canonical Wnt/β-catenin pathway was examined because of its important role in osteogenesis and bone formation [25,26]. As previously reported by our group [19], hepcidin deficiency caused body iron accumulation, and iron is known to cause oxidative stress through the Fenton reaction [27]. Moreover, oxidative stress is known to affect the canonical Wnt/β-catenin pathway via FOXO3a [28]. Thus, we tested whether hepcidin deficiency affected the canonical Wnt/β-catenin pathway. β-catenin protein expression was not significantly different in the bone tissues from WT and Hepcidin-KO mice as assessed by Western blot (Fig. 4A). However, co-immunoprecipitation analysis showed that β-catenin combined more with TCF4/TCF7L2 (a factor of the TCF/LEF family) in the bone tissues from WT mice, and β-catenin combined more with FOXO3a (a factor of the Forkhead box O family) in the bone tissues from Hepcidin-KO mice (Fig. 4B). Therefore, reduced osteoblastic differentiation and activity caused by hepcidin deficiency may be because of diverting β-catenin binding from TCF4/TCF7L2 to FOXO3a in the absence of hepcidin, thus affecting the canonical Wnt/β-catenin pathway.

AAV-mediated delivery of FOXO3a-RNAi alleviates bone loss in hepcidin-KO mice

To confirm the *in vivo* function of FOXO3a in bone metabolism, we examined the effect of AAV-mediated delivery of FOXO3a-RNAi on the bone mass of Hepcidin-KO mice. When FOXO3a-RNAi was delivered by tail vein administration, the bone loss phenotype in Hepcidin-KO mice was alleviated after 1 month (Fig. 5A and 5B). Bone morphometric analysis showed an increase in BMD (Fig. 5C), BV/TV (Fig. 5D) and Tb.N (Fig. 5E) and a decrease in Tb.Sp (Fig. 5F) after FOXO3a-RNAi

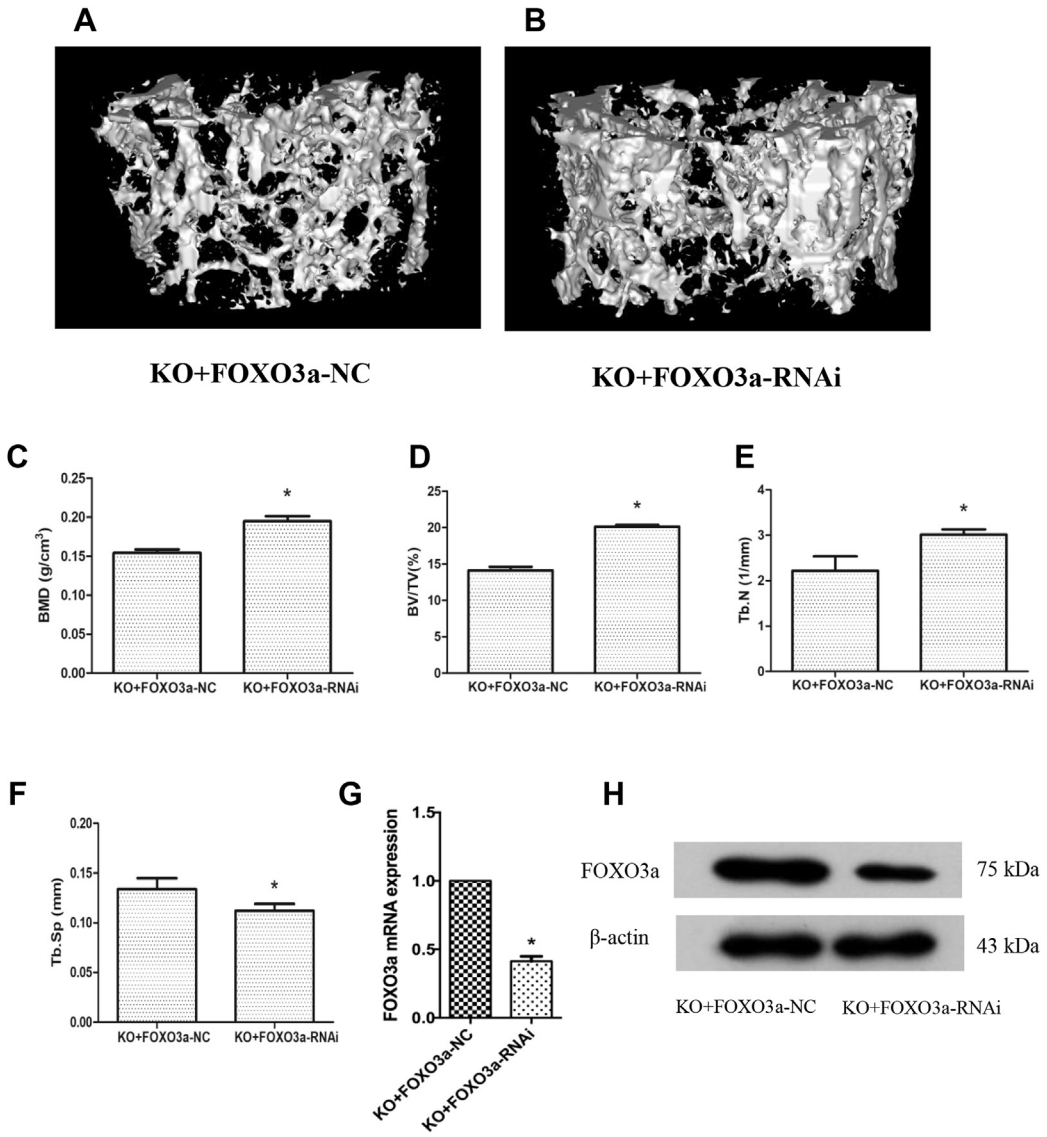

Figure 5. AAV-mediated delivery of FOXO3a-RNAi alleviates bone loss in Hepcidin-KO mice. (A-F) Micro-CT of the trabecular bone of the distal femur from Hepcidin-KO mice treated with either FOXO3a-RNAi or FOXO3a-NC. (A) Representative three-dimensional image of the trabecular bone of the distal femur from Hepcidin-KO mice treated with FOXO3a-NC; (B) representative three-dimensional image of the trabecular bone of the distal femur from Hepcidin-KO mice treated with FOXO3a-RNAi; (C) bone mineral density (BMD) of the distal femur from Hepcidin-KO mice treated with FOXO3a-NC and FOXO3a-RNAi; (D) bone volume to total volume (BV/TV) ratio of the distal femur from Hepcidin-KO mice treated with FOXO3a-NC and FOXO3a-RNAi; (E) trabecular number (Tb.N) of the distal femur from Hepcidin-KO mice treated with FOXO3a-NC and FOXO3a-RNAi; (F) trabecular separation (Tb.Sp) of the distal femur from Hepcidin-KO mice treated with FOXO3a-NC and FOXO3a-RNAi; (G) mRNA expression of FOXO3a in the femur of Hepcidin-KO mice treated with FOXO3a-NC and FOXO3a-RNAi; (H) protein expression of FOXO3a in the femur of Hepcidin-KO mice treated with FOXO3a-NC and FOXO3a-RNAi. Data are means ± SD from six mice. *$p < 0.05$ by Student t test. AVV = adeno-associated virus; WT = wild type; Hepcidin-KO = hepcidin knockout; Micro-CT = microcomputed tomography; FOXO3a = Forkhead box O3a.

administration, whereas Tb.Th was not altered after FOXO3a-RNAi administration (data not shown). In addition, we confirmed decreased expression of FOXO3a mRNA (Fig. 5G) and protein (Fig. 5H) in bone tissues after FOXO3a-RNAi delivery.

Therefore, we confirmed the role of FOXO3a in hepcidin deficiency–induced bone loss and provide a possible approach to treat hepcidin deficiency–induced bone loss by inhibiting FOXO3a.

Discussion

As previously reported [19], hepcidin deficiency causes body iron accumulation, possibly via its unique role in regulating body iron metabolism. Hepcidin is an endogenous hormone peptide that is the main regulator of iron homeostasis [14–16]. Hepcidin can bind to ferroportin, which is thought to be the only export protein located on enterocytes. The combination of hepcidin with ferroportin could reduce ferroportin activity by causing internalisation, which in turn inhibits iron uptake and transfer from the gastrointestinal system to the circulatory system, thus leading to decreased body iron content [17,18]. Therefore, hepcidin-deficient mice exhibit body iron accumulation, making it an optimal model for studying iron accumulation-induced osteoporosis. Clinical studies showed that hepcidin levels were markedly decreased in patients with osteoporosis [29]. Animal studies of mice showed similar results when hepcidin was absent [19,20].

Iron accumulation is known to produce oxidative stress through the Fenton reaction [27] and has recently been considered an independent risk factor for osteoporosis [3]. In this study, we found that hepcidin deficiency affected osteoblastic differentiation and activity, rather than

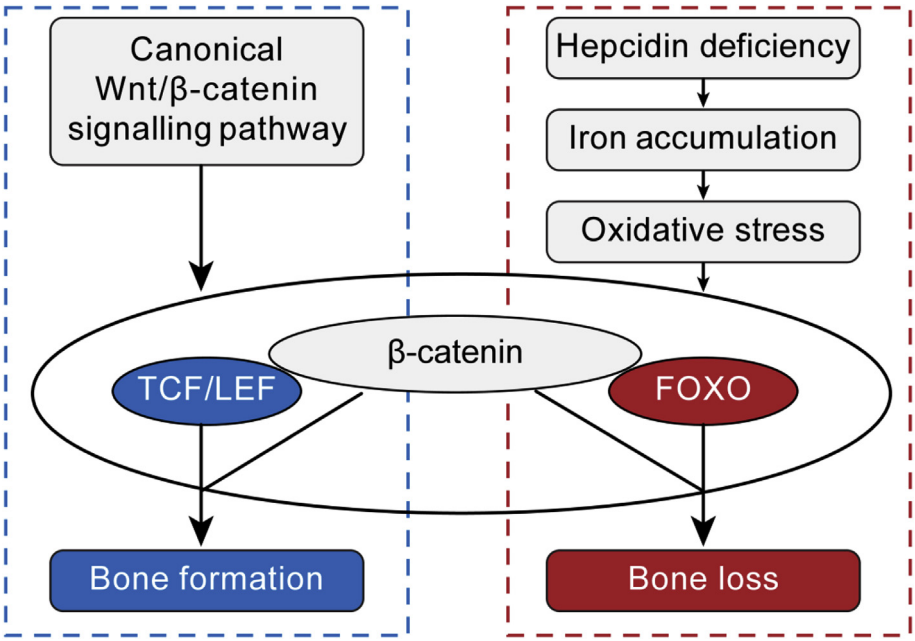

Figure 6. Schematic overview of the role of FOXO3a in hepcidin deficiency-induced bone loss. FOXO3a = Forkhead box O3a.

osteoclastic differentiation and activity. This is consistent with previous reports [30–32] that iron accumulation can inhibit either osteoblastogenesis or osteoblastic function directly. Furthermore, it was reported that when iron accumulates, bone mesenchymal stem cell apoptosis is induced, and osteoblast autophagy and apoptosis are increased [33–35]. Regarding signalling pathways, the hedgehog pathway and sphingosine-1-phosphate/sphingosine-1-phosphate receptor signalling axis were found to be involved in the reduced osteoblastic function associated with iron accumulation [36,37].

Interestingly, ion accumulation is also reported to stimulate osteoclastogenesis [38,39]. The NF-κB signalling pathway and transient receptor potential vanilloid type 1 channels were found to be involved in iron accumulation-related osteoclastic function [40,41]. This is different from our study results and indicates different roles of hepcidin deficiency and iron accumulation in bone metabolism that should be investigated.

Iron accumulation–induced oxidative stress has recently been shown to divert β-catenin from T-cell factor to FOXO, thus affecting the canonical Wnt/β-catenin pathway and leading to bone loss [28]. TCF4/TCF7L2 (a factor of the TCF/LEF family) and FOXO3a (a factor of the Forkhead box O family) were used in this study because of previous reports [28,42]. In this study, we found that under normal conditions, β-catenin combined more with TCF4/TCF7L2, a factor of the TCF/LEF family, leading to downstream transcription and bone formation. Under hepcidin deficiency conditions, β-catenin combined more with FOXO3a, thus inhibiting the canonical Wnt/β-catenin pathway and causing bone loss. The results are consistent with previous reports that highlighted the role of FOXO in bone formation [28,43,44] and might account for the reduced osteoblastic differentiation and activity after hepcidin deficiency.

Importantly, because of the lack of a neutralised FOXO3a antibody, we used AAV-mediated FOXO3a-RNAi to inhibit FOXO3a transcription. We then observed whether inhibiting FOXO3a expression is good for the bone status of hepcidin-KO mice. In line with our expectations, delivery of AAV-mediated FOXO3a-RNAi via tail vein administration significantly alleviated bone loss in hepcidin-KO mice after 1 month.

In conclusion, hepcidin deficiency may cause bone loss by interfering with the canonical Wnt/β-catenin pathway via FOXO3a (Fig. 6), thus providing a possible approach to treat hepcidin deficiency–caused bone loss by inhibiting FOXO3a.

Author contributions

Study design was contributed by G.L., J.W., X.M., and Y.X. Micro-CT analyses was carried out by H.Z. and A.W. Data analysis and interpretation was done by G.L., J.W., F.Y., and B.C. Tail vein administration of FOXO3a-RNAi was done by H.Z. and Y.G. Manuscript drafting was carried out by G.L., J.W., and Y.G. Study supervision was done by X.M. and Y.X. All authors reviewed and approved the final manuscript.

Funding

This study was funded by the National Natural Science Foundation of China (81500680; 81874018), the Jiangsu Province Youth Elite Programme (QNRC2016878), and the Advantage Discipline Group of The Second Affiliated Hospital of Soochow University (XKQ2015001).

Research involving animals ethical approval

All procedures performed in studies involving animals were in accordance with the ethical standards of the Ethics Committee of Soochow University (ECSU-201800093).

Conflicts of Interest

All authors state that they have no conflicts of interest.

Acknowledgements

This work was supported by the National Natural Science Foundation of China (81500680; 81874018), the Jiangsu Province Youth Elite Programme (QNRC2016878), and the Advantage Discipline Group of The Second Affiliated Hospital of Soochow University (XKQ2015001).

Appendix A. Supplementary data

Supplementary data to this article can be found online at https://doi.org/10.1016/j.jot.2020.03.012.

References

[1] Weinberg ED. Iron loading: a risk factor for osteoporosis. Biometals 2006;19:633–5.
[2] Weinberg ED. Role of iron in osteoporosis. Pediatr Endocrinol Rev 2008;6(Suppl 1): 81–5.
[3] Li GF, Pan YZ, Sirois P, Li K, Xu YJ. Iron homeostasis in osteoporosis and its clinical implications. Osteoporos Int 2012;23:2403–8.
[4] Kim BJ, Ahn SH, Bae SJ, Kim EH, Lee SH, Kim HK, et al. Iron overload accelerates bone loss in healthy postmenopausal women and middle-aged men: a 3-year retrospective longitudinal study. J Bone Miner Res 2012;27:2279–90.
[5] Kim BJ, Lee SH, Koh JM, Kim GS. The association between higher serum ferritin level and lower bone mineral density is prominent in women >/=45 years of age (KNHANES 2008-2010). Osteoporos Int 2013;24:2627–37.
[6] Ahn SH, Lee S, Kim H, Lee SH, Kim BJ, Koh JM. Higher serum ferritin level and lower femur neck strength in women at the stage of bone loss (>/= 45 years of age): the Fourth Korea National Health and Nutrition Examination Survey (KNHANES IV). Endocr Res 2016;41:334–42.
[7] Jian J, Pelle E, Huang X. Iron and menopause: does increased iron affect the health of postmenopausal women. Antioxidants Redox Signal 2009;11:2939–43.
[8] Zwart SR, Morgan JL, Smith SM. Iron status and its relations with oxidative damage and bone loss during long-duration space flight on the International Space Station. Am J Clin Nutr 2013;98:217–23.
[9] Qu ZH, Zhang XL, Tang TT, Dai KR. Promotion of osteogenesis through beta-catenin signaling by desferrioxamine. Biochem Biophys Res Commun 2008;370:332–7.
[10] Zhang W, Li G, Deng R, Deng L, Qiu S. New bone formation in a true bone ceramic scaffold loaded with desferrioxamine in the treatment of segmental bone defect: a preliminary study. J Orthop Sci 2012;17:289–98.
[11] Kusumbe AP, Ramasamy SK, Adams RH. Coupling of angiogenesis and osteogenesis by a specific vessel subtype in bone. Nature 2014;507:323–8.
[12] Poggi M, Sorrentino F, Pugliese P, Smacchia MP, Daniele C, Equitani F, et al. Longitudinal changes of endocrine and bone disease in adults with beta-thalassemia major receiving different iron chelators over 5 years. Ann Hematol 2016;95: 757–63.
[13] Hou JM, Xue Y, Lin QM. Bovine lactoferrin improves bone mass and microstructure in ovariectomized rats via OPG/RANKL/RANK pathway. Acta Pharmacol Sin 2012; 33:1277–84.
[14] Ganz T. Hepcidin–a regulator of intestinal iron absorption and iron recycling by macrophages. Best Pract Res Clin Haematol 2005;18:171–82.
[15] Mena NP, Esparza AL, Nunez MT. Regulation of transepithelial transport of iron by hepcidin. Biol Res 2006;39:191–3.
[16] Collins JF, Wessling-Resnick M, Knutson MD. Hepcidin regulation of iron transport. J Nutr 2008;138:2284–8.
[17] Nemeth E, Tuttle MS, Powelson J, Vaughn MB, Donovan A, Ward DM, et al. Hepcidin regulates cellular iron efflux by binding to ferroportin and inducing its internalization. Science 2004;306:2090–3.
[18] De Domenico I, Kushner JP. Reconstitution of normal hepcidin expression in Hfe-deficient mice after liver transplantation: a new role of HFE in Kupffer cells. Gastroenterology 2010;139:25–7.
[19] Shen GS, Yang Q, Jian JL, Zhao GY, Liu LL, Wang X, et al. Hepcidin 1 knockout mice display defects in bone microarchitecture and changes of bone formation markers. Calcif Tissue Int 2014;94:632–9.
[20] Sun L, Guo W, Yin C, Zhang S, Qu G, Hou Y, et al. Hepcidin deficiency undermines bone load-bearing capacity through inducing iron overload. Gene 2014;543:161–5.
[21] Jia P, Xu YJ, Zhang ZL, Li K, Li B, Zhang W, et al. Ferric ion could facilitate osteoclast differentiation and bone resorption through the production of reactive oxygen species. J Orthop Res 2012;30:1843–52.
[22] Takahashi N, Muto A, Arai A, Mizoguchi T. Identification of cell cycle-arrested quiescent osteoclast precursors in vivo. Adv Exp Med Biol 2010;658:21–30.
[23] Soleimani M, Nadri S. A protocol for isolation and culture of mesenchymal stem cells from mouse bone marrow. Nat Protoc 2009;4:102–6.
[24] Knierim E, Hirata H, Wolf NI, Morales-Gonzalez S, Schottmann G, Tanaka Y, et al. Mutations in subunits of the activating signal cointegrator 1 complex are associated with prenatal spinal muscular atrophy and congenital bone fractures. Am J Hum Genet 2016;98:473–89.
[25] Krishnan V, Bryant HU, Macdougald OA. Regulation of bone mass by Wnt signaling. J Clin Invest 2006;116:1202–9.
[26] Kim JH, Liu X, Wang J, Chen X, Zhang H, Kim SH, et al. Wnt signaling in bone formation and its therapeutic potential for bone diseases. Ther Adv Musculoskelet Dis 2013;5:13–31.
[27] Winterbourn CC. Toxicity of iron and hydrogen peroxide: the Fenton reaction. Toxicol Lett 1995;82-83:969–74.
[28] Almeida M, Han L, Martin-Millan M, O'Brien CA, Manolagas SC. Oxidative stress antagonizes Wnt signaling in osteoblast precursors by diverting beta-catenin from T cell factor- to forkhead box O-mediated transcription. J Biol Chem 2007;282: 27298–305.
[29] Liu B, Liu C, Zhong W, Song M, Du S, Su J. Reduced hepcidin level features osteoporosis. Exp Ther Med 2018;16:1963–7.
[30] Yang Q, Jian J, Abramson SB, Huang X. Inhibitory effects of iron on bone morphogenetic protein 2-induced osteoblastogenesis. J Bone Miner Res 2011;26: 1188–96.
[31] He YF, Ma Y, Gao C, Zhao GY, Zhang LL, Li GF, et al. Iron overload inhibits osteoblast biological activity through oxidative stress. Biol Trace Elem Res 2013; 152:292–6.
[32] Doyard M, Chappard D, Leroyer P, Roth MP, Loreal O, Guggenbuhl P. Decreased bone formation explains osteoporosis in a genetic mouse model of hemochromatosiss. PloS One 2016;11:e0148292.
[33] Liu F, Zhang WL, Meng HZ, Cai ZY, Yang MW. Regulation of DMT1 on autophagy and apoptosis in osteoblast. Int J Med Sci 2017;14:275–83.
[34] Tian Q, Wu S, Dai Z, Yang J, Zheng J, Zheng Q, et al. Iron overload induced death of osteoblasts in vitro: involvement of the mitochondrial apoptotic pathway. PeerJ 2016;4:e2611.
[35] Yuan Y, Xu F, Cao Y, Xu L, Yu C, Yang F, et al. Iron accumulation leads to bone loss by inducing mesenchymal stem cell apoptosis through the activation of Caspase 3. Biol Trace Elem Res 2019;187:434–41.
[36] Doyard M, Fatih N, Monnier A, Island ML, Aubry M, Leroyer P, et al. Iron excess limits HHIPL-2 gene expression and decreases osteoblastic activity in human MG-63 cells. Osteoporos Int 2012;23:2435–45.
[37] Peltier L, Bendavid C, Cavey T, Island ML, Doyard M, Leroyer P, et al. Iron excess upregulates SPNS2 mRNA levels but reduces sphingosine-1-phosphate export in human osteoblastic MG-63 cells. Osteoporos Int 2018;29:1905–15.
[38] Wang L, Fang B, Fujiwara T, Krager K, Gorantla A, Li C, et al. Deletion of ferroportin in murine myeloid cells increases iron accumulation and stimulates osteoclastogenesis in vitro and in vivo. J Biol Chem 2018;293:9248–64.
[39] Xiao W, Beibei F, Guangsi S, Yu J, Wen Z, Xi H, et al. Iron overload increases osteoclastogenesis and aggravates the effects of ovariectomy on bone mass. J Endocrinol 2015;226:121–34.
[40] Wang X, Chen B, Sun J, Jiang Y, Zhang H, Zhang P, et al. Iron-induced oxidative stress stimulates osteoclast differentiation via NF-kappaB signaling pathway in mouse model. Metab Clin Exp 2018;83:167–76.
[41] Rossi F, Perrotta S, Bellini G, Luongo L, Tortora C, Siniscalco D, et al. Iron overload causes osteoporosis in thalassemia major patients through interaction with transient receptor potential vanilloid type 1 (TRPV1) channels. Haematologica 2014;99: 1876–84.
[42] Nagano A, Arioka M, Takahashi-Yanaga F, Matsuzaki E, Sasaguri T. Celecoxib inhibits osteoblast maturation by suppressing the expression of Wnt target genes. J Pharmacol Sci 2017;133:18–24.
[43] Iyer S, Han L, Ambrogini E, Yavropoulou M, Fowlkes J, Manolagas SC, et al. Deletion of FoxO 1, 3, and 4 in osteoblast progenitors attenuates the loss of cancellous bone mass in a mouse model of type 1 diabetes. J Bone Miner Res 2017; 32:60–9.
[44] Iyer S, Ambrogini E, Bartell SM, Han L, Roberson PK, de Cabo R, et al. FOXOs attenuate bone formation by suppressing Wnt signaling. J Clin Invest 2013;123: 3409–19.